RSC Advances

ROYAL SOCIETY OF CHEMISTRY

www.rsc.org/advances

Graphical Abstract

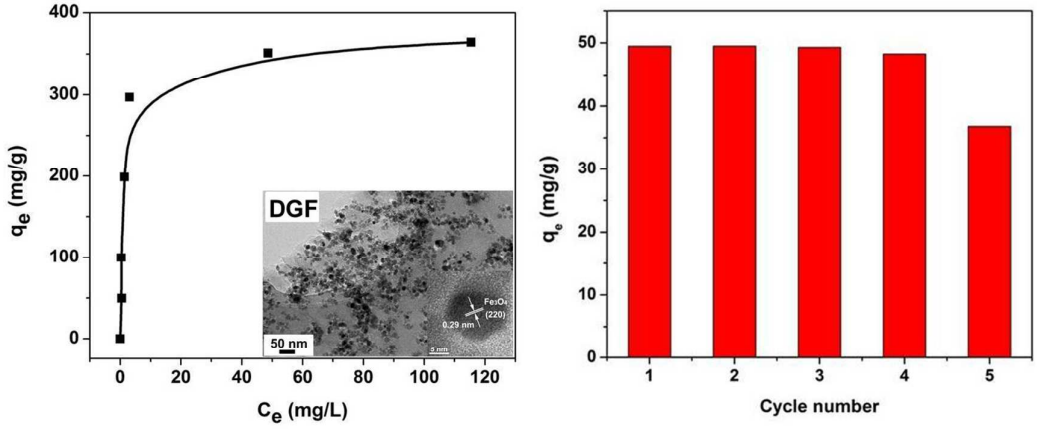

The polydopamine-functionalized graphene-Fe_3O_4 (DGF) nanocomposites have been prepared by a simple solution mixing method. The obtained DGF has high adsorption capacity of 365.39 mg/g and easy-separation ability.

Cite this: DOI: 10.1039/c0xx00000x

www.rsc.org/xxxxxx

ARTICLE TYPE

Preparation of polydopamine-functionalized graphene/Fe_3O_4magneticcompositeswith high adsorption capacities

Xiaofang Han, Ling Zhang, * and Chunzhong Li *

Received (in XXX, XXX) Xth XXXXXXXXX 20XX, Accepted Xth XXXXXXXXX 20XX

DOI: 10.1039/b000000x

Here we report a simple solution mixing method to prepare polydopamine-functionalized graphene-Fe_3O_4 (DGF) nanocomposites with high adsorption capacities and easy-separation ability. Water-soluble Fe_3O_4 particles are firmly deposited on the surfaces of the graphene oxide (GO) via the electrostatic and hydrogen interactions. The interaciton between the GO and Fe_3O_4 particles could prevent graphenenanosheets from restacking and Fe_3O_4 particles from agglomeration. The introduction of dopamine to functionalize the GO can not only reduce the GO but also endow abundant chemical groups. The existence of polydopamine affords more active sites for adsorption and further enhances the interaction of GO and Fe_3O_4 particles to obtain adsorbent materials with stable structure. The adsorption capacity of DGF nanocomposites for methylene blue (MB) is 365.39 mg/g, which is much higher than that of graphene-Fe_3O_4 (GF) nanocomposite. Simultaneously, the DGF nanocomposites can be easily removed from polluted water after adsorption for MB by using magnetic field, which is very important for the water conservation.

1. Introduction

Graphene is a new type of two-dimensional carbon nanostructure with excellent properties, such as extraordinary mechanical, electrical and thermal properties. Their unique chemical structures and inspiring properties make it a promising material in many potential applications including lithium ion batteries, supercapacitors, sensors, nanocomposites, and so on.[1-3] Also, its high specific surface areas make graphene an excellent choice for adsorbents of organic contaminants for wastewater treatment. However, how to achieve high adsorption capacities still has some technological challenges for graphene due to their relatively low density of surface functional groups and easy stacking of graphene sheets during reduction.[4]

A large amount of researchers are targeted to overcome these challenges. One attractive and efficient way to improve the dispersion of graphene is to use polydopamine (PDA) as the adhesive coatings on two-dimensional nanofillers and endow graphene new functionality. Dopamine (or 3,4-dihydroxyphenethylamine), which contains catechol and amine groups,[5-6] could self-polymerization under room temperature to produce PDA.[7] PDA could adhere to the surface of many organic and inorganic substance strongly by forming covalent band and many other intermolecular interactions, such as hydrogen bond. Yang et al. reported that dopamine makes each graphene sheet sandwiched between two PDA, which prevent the agglomeration of graphene sheets so that the specific surface area could be enhanced.[8] Furthermore, there are many active groups on the surface of PDA，which endow it the secondary reaction ability.[9-11] On the other hand, depositing nanoparticles on graphene oxide (GO) sheets can also prevent graphenenanosheets from restacking and endow new functionality to this 2D carbon nanomaterials. It is reported that Fe_3O_4,[12] TiO_2,[13] Co_3O_4[14-15] could be deposited on GO sheets. It is well-known that Fe_3O_4 nanoparticles could be easily separated by an external magnetic field owing to their unique superparamagnetism effect.[16-17] The hybrid of graphene and Fe_3O_4 could effectively combine the adsorption and magnet-separation ability and represent a potential class of adsorbents for wastewater treatment.[18-21] Zhang et al. fabricated high crystalline Fe_3O_4-graphene composites by one-step thermolysis of iron-organic complex and graphene oxide sheets under an oxygen-free condition, which show a high efficiency of removing methylene blue (MB) molecule.[20] Xie et al. prepared a superparamagnetic grapheme oxide-Fe_3O_4 hybrid composite by the deposition of amino-functionalized Fe_3O_4 particles on the grapheme oxide sheets, showing the adsorption capacities of 171.3 mg/g for MB.[21] Nevertheless, the combination of graphene and Fe_3O_4 by hydrothermal or other chemical processes is complicated compared to physical procedures,[20-23] which extremely limits the application of Fe_3O_4/grapheme composites in wastewater treatment.

Herein, polydopamine-functionalized graphene-Fe_3O_4nanocomposites (DGF) are successfully prepared by a facile solution mixing process. Positive water-soluble Fe_3O_4 are chosen to deposit onto negative GO sheets by electrostatic adsorption which is an easy operation process. The interaciton between the GO and Fe_3O_4 particles could prevent graphene nanosheets from restacking and Fe_3O_4 particles from agglomeration. Furthermore, dopamine is used to functionalize the GO-Fe_3O_4, which plays many functional roles as follows: 1) reduce the GO into graphene; 2) coat on the surfaces of graphene-

Fe_3O_4 and prevent the restacking of rGO sheets; 3) enhance the interaction of GO and Fe_3O_4 particles to obtain stable structure; 4) endow abundant chemical groups for adsorption. The DGF hybrids not only have excellent adsorptive properties, but also could be separated quickly by an external magnetic field instead of the time-consuming process, such as sedimentation, centrifugation and filtration.[18-19] The results showed that the DGF hybrids could become one of promising candidates for water purification due to its high adsorption capacity and convenient magnetic separation.

2. Experimental section

2.1Synthesis of polydopamine-graphene-Fe_3O_4 (DGF)

GO was prepared from natural graphite by the modified Hummer's method.Natural graphite (1 g) and $NaNO_3$ (1 g) were grinded, and then the mixtures were transferred to 1000 mL flask. Concentrated H_2SO_4 (60 mL) was slowly dropped into flask and stirred in an ice bath for 20 min. Further, $KMnO_4$ (6 g) was slowly added within 10 min. The mixture was further stirred for 5 days at room temperature. Deionized water (150 mL, 50 ℃-60 ℃) was slowly added, and then stirred for 2 h. After that, 30% H_2O_2 (10 mL) was dropped to reduce the residual until the slurry turned golden yellow. After washed with HCl solution and water, the brown solutions were diluted and ultrasonicated to become a brown-yellow, homogeneous dispersion of GO. Water-soluble Fe_3O_4-OH_2^+ nanoparticle solutions were synthesized according to the method reported previously.[24]

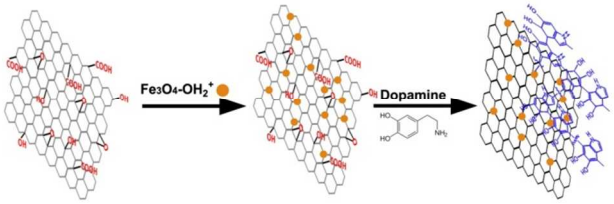

Scheme 1 Illustration for the synthesis of DGF hybrids

The fabrication process of DGF hybrids is illustrated in scheme 1. Dopamine (6.25 mg) was added into the mixture of GO (12.50 mg) aqueous dispersions and Fe_3O_4 (6.25 mg) nanoparticle solutions. Then the pH was adjusted to about 7.0. The volume of the solution was controlled to be 5 mL. When the mixture was heated at 60 ℃ for 24 h without any disturbance, the dark DGF solution was obtained. The DGF could be separated by a magnetic field for further use. By contrast, the preparation of graphene-Fe_3O_4 (GF) nanocomposites was similar to DGF without dopamine.

2.2Materials characterizations

The as-synthesized materials were characterized by X-ray diffraction (XRD), performed on a Rigaku D/max 2550VB/PC diffractometer at room temperature. The patterns were recorded over the angular range 3-80° (2θ), using Cu Kα radiation (λ = 0.154056 nm) with working voltage and current of 40 kV and 100 mA, respectively. High-resolution transmission electron microscopy (HRTEM: JEOL JEM-2100), and Field emission scanning electron microscopy (FE-SEM: HITACHI S-4800) with energy dispersive X-ray spectroscopy (EDS) were used to characterize the morphology microstructure. The Raman spectra were obtained using a spectrometer (Via+Reflex) using an excitation laser wavelength of 514 nm. Magnetic properties were measured at room temperature on a vibrating sample magnetometer (VSM, lakeshore7407) at room temperature with an applied magnetic field from -18 kOe to 18 kOe.

2.3 Adsorption and desorptionexperiments

Adsorption experiments were carried out in glass beaker at 25 ℃. 25 mL of MB solution of a known initial concentration was stirred with 25 mg of magnetic DGF. After magnetic separation using the permanent magnet, the equilibrium concentrations of dyes were measured with a UV-vis spectrophotometer at a wavelength of 664 nm. The adsorption capacity of MB on the adsorbents was evaluated according to the equation:

$$q = \frac{(C_0 - C_e)V}{W}$$

where q (mg/g) is the amount of MB adsorbed onto the adsorbents at equilibrium, C_0 (mg/L) and C_e (mg/L) are the initial and equilibrated MB concentrations, respectively, V (L) is the volume of solution added, and W (g) is the mass of the adsorbent.

For the desorption study, 25 mg of DGF adsorbent was added to 25 mL MB solution with a concentration of 50 mg/L, and the mixture was stirred at ambient temperature for 20 min. After the magnetic separation, the supernatant dye solution was discarded and the adsorbent was separated. Then, 25 mL ethanol was added to the adsorbent and stirred for 20 min. The adsorbent was collected using a magnet and reused. The supernatant solutions were measured by UV-vis spectra. The cycles of absorption-desorption processes were successively conducted 5 times.

3. Results and discussion

3.1 Morphology and composition

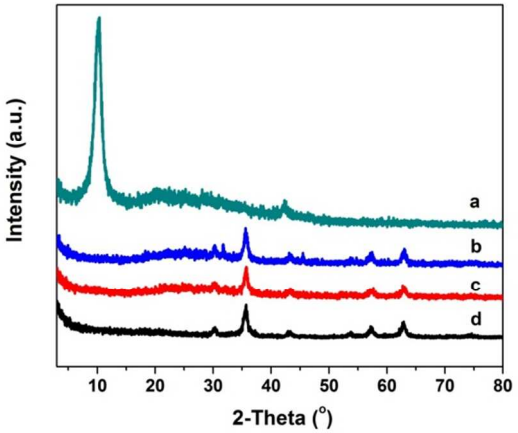

Fig. 1XRD patterns of (a) GO, (b) DGF, (c) GF and (d) Fe_3O_4

Fig. 1 shows the XRD patterns of GO, DGF, GF, Fe_3O_4. As shown in Fig. 1a, a sharp diffraction (002) peak at 2Θ = 10.26° is clearly observed, indicating that nature graphite is converted into GO after acute oxidation by the modified Hummer's method. The corresponding d-spacing of (002) peak is 0.86 nm, much higher than that of graphite (~ 0.34 nm).[19]This may be attributed to the

formation of oxygen-containing functional groups on the graphite surface. Fig. 1d shows the typical XRD pattern of as-prepared Fe_3O_4. The diffraction peaks at 30.16°, 35.60°, 43.22°, 53.78°, 57.32° and 62.92° are corresponding to the (220), (311), (400), (422), (511) and (440) planes of Fe_3O_4 (JCPDS no. 65-3107). Compared to Fe_3O_4, DGF and GF show all the diffraction peaks of Fe_3O_4 without the peak of GO at 2Θ = 10.26°. The phenomenon of the disappearance of the (002) peak of GO is also reported by other groups. It may be attributed to the strong peaks of Fe_3O_4 which overwhelm the weak GO peaks. On the other hand, the presence of Fe_3O_4 and PDA reduces the aggregation of graphene sheets, which results in more monolayer graphene, resulting in the formation of broad peak at $2\Theta = 25°$.[25-26]

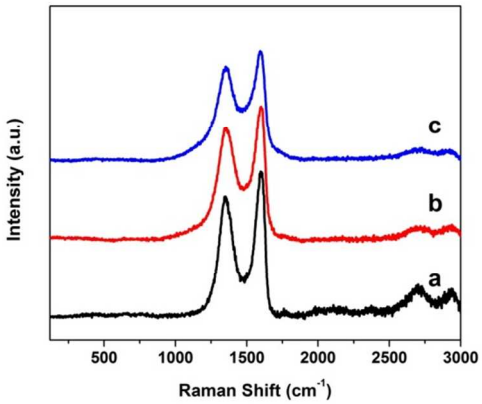

Fig.2 Raman spectra of (a) GO, (b) DGF and (c) GF composite

Raman is a very powerful and valuable technique to characterize carbon materials. The Raman spectrum of graphene is usually characterized by two main features, the G band at 1575 cm^{-1} is the indication of the E_{2g} phonon of C sp^2 atoms in a 2-dimensional hexagonal lattice, while the D band at 1350 cm^{-1} arises from a breathing mode of κ-point photons of A1g symmetry.[27-28] The intensity ratio of D band to G band (I_D/I_G) is usually used as a measure of the disorder. Fig. 2 shows the Raman spectra of GO, DGF and GF. The I_D/I_G of GF (0.84) shows a similar value as compared with that of GO (0.83), indicating the non-destruction of GO structure by the electrostatic adhesion between GO and Fe_3O_4-OH_2^+. Further, DGF has a higher I_D/I_G value of 0.87. This may be attributed to the functional groups on the surface of dopamine, which increases the edge defect of DGF by forming adhesive layers on graphene.

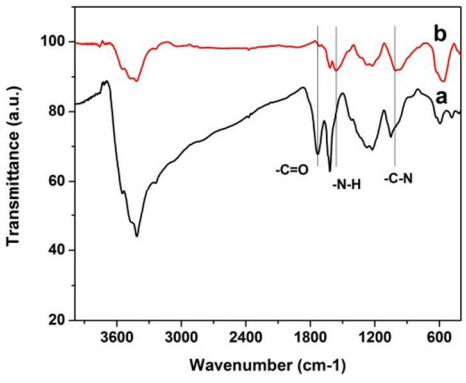

Fig. 3FTIR spectra of (a) GO and (b) DGF

The successful incorporation of polydopamine into GO was further confirmed by FTIR spectroscopy. Fig. 3 displays the FTIR spectrum of GO and DGF. The bands of GO at 1729 cm^{-1} and 3414 cm^{-1} indicates the existence of the large amount of carbonyl group (C=O) and hydroxyl group (-OH) on the surface of GO. Furthermore, the band of aromatic double bond (C=C) stretching could be visible at 1618 cm^{-1}. After combination with dopamine and Fe_3O_4, the wide peak at 3414 cm^{-1} is significantly decreased and the peak of C=O at 1729 cm^{-1} almost disappeared in DGF. These are mainly attributed to the removal of oxygen functionalities from GO as a result of the reduction effect of dopamine. In addition, the peaks at 1557 cm^{-1} and 1005 cm^{-1} are corresponding to the N-H and C-N stretching vibration, respectively. The FTIR data suggests the successful introduction of dopamine in DGF hybrid.

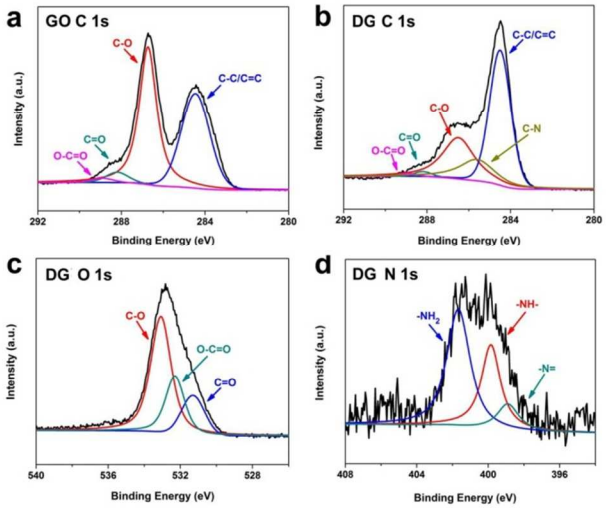

Fig. 4XPS spectra for (a) C 1s peak of GO and (b) C 1s, (c) O 1s, (d) N 1s peaks of DG

To further identify the chemical bonding information in the composites, the GO and polydopamine-graphene (DG) samples were examined by XPS. As shown in Fig. 4a, the C 1s peak of GO is deconvoluted into four components with binding energy at 284.5, 286.7, 288.2 and 288.9 eV, corresponding to C-C/C=C, C-O, C=O and O-C=O species, respectively. The C 1s spectra of DG are similar to GO, but the intensities of the peaks for the oxygen functional groups decreased significantly, while the peak of C-C/C=C becomes dominant. This suggests most GO was reduced to graphene by dopamine. The O 1s spectra of DG can be divided into three components of C-O (531.3 eV), O-C=O (532.3 eV) and C=O (533.1 eV), which correspond to the spectra of C 1s (Fig. 4c). Besides, a new peak of N 1s emerges in DG, which proves the existence of PDA on graphene sheets. This peak could be deconvoluted into three components, whose binding energies at 398.9 eV, 399.9 eV and 401.7 eV correspond to N-R, R-NH-R and R-NH_2 groups respectively (Fig. 4d). The presence of secondary amine in DG suggests that dopamine was spontaneously polymerized PDA during its oxidation by GO.[29]The conclusion of DG could indirectly reflect the polymerization of dopamine on the surface of graphene and

Fe_3O_4 and the reduction of GO by dopamine.

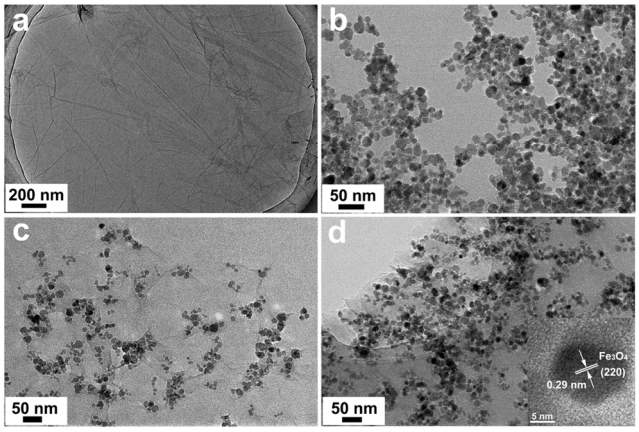

Fig. 5TEM images of (a) GO, (b) Fe_3O_4, (c) GF hybrid, and (d) DGF hybrid and inset is HR-TEM image of Fe_3O_4

The morphology and structures of as-prepared GO, Fe_3O_4, DGF and GF are fully detected by TEM and HRTEM observation. The representative TEM image of GO sample is depicted in Fig. 5a. The obtained GO samples are transparent and have a crumpled and rippled structure. This can attributed to the deformation upon the exfoliation process. Fig. 5b shows the TEM image of pure Fe_3O_4 nanoparticles, which possesses a narrow particle size distribution ranging from 16-22 nm. Moreover, with a combination of GO sheets and Fe_3O_4 nanoparticles, as shown in Fig. 5c and d, the magnetite particles are firmly anchored on the surfaces of GO substrates because of the electrostatic interaction between negative GO and positive Fe_3O_4. The existence of graphenenanosheets substrate could effectively prevent the nanoparticles from agglomeration and endow a good dispersion of these magnetite nanoparticles. The morphology of DGF composites has no apparent difference with comparison to that of GF. However, it should be emphasized that, with the presence of dopamine, more magnetite particles are anchored onto the graphene (TEM image in Fig. 5d) owing to the bridge-like linking of polydopamine with the abundant groups (i.e., hydroxyl and amino-group). Further, the corresponding HRTEM image in Fig. 5d reveals that the obtained Fe_3O_4 nanoparticles have a good crystallinity and a lattice spacings of 0.29 nm, which are in good agreement with the (200) planes of Fe_3O_4.[21] Therefore, it is believed that such a perfect DGF structure would have high adsorption performance as a result of the good dispersion of nanoparticles and nanosheets, abundant groups from polydopamine and the excellent magnetic response ability.

3.2 Adsorption Properties.

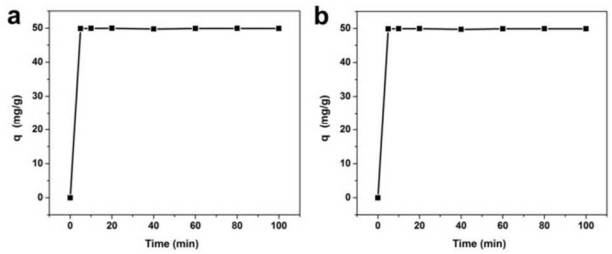

Fig. 6 The effect of contact time on the adsorption of 50 mg/L MB onto (a) GF and (b) DGF

The adsorption properties of the as-prepared samples toward dyes MB from aqueous solution are investigated in detail. Fig. 6 shows the effect of contact time on the amount of dye adsorbed on GF and DGF at an initial concentration of 50 mg/L of MB. It can be seen that the adsorption process is very fast and it could attain equilibrium within 5 min. The extremely short equilibrium time suggests the high adsorption efficiency of graphene composites. The adsorption ability of DGF and GF is above 49 mg/g, the corresponding removal efficiency is close to 100%. Such an excellent adsorption capability and fast adsorption ability may be attributed to the π-π and electrostatic interaction between aromatic rings of MB molecules and graphene.[18-19]Besides, the Fe_3O_4nanoparicles could disperse on graphene uniformly and prevent graphene sheets from agglomeration. This enhanced contact area between graphene and MB, which is favorable to the adsorption of MB.

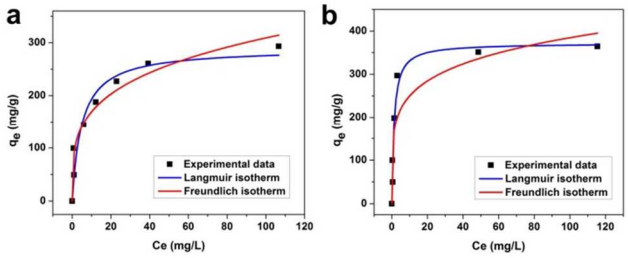

Fig. 7 Isotherms of MB adsorption on the (a) GF and (b) DGF composites (temperature: 25 ℃; contact time: 20 min)

Fig. 7 shows the adsorption isotherm for MB with different initial concentration on GF and DGF. The adsorption abilities of DGF and GF increase with the increasing initial concentration of MB and finally reached the saturation. The saturated adsorption capabilities for GF and DGF are almost 293.37 mg/g and 365.39 mg/g. It can be clearly seen that the adsorption capability of DGF is much better than that of GF. GF shows a higher residual MB concentration than DGF when initial MB concentration is above 100 mg/L. The high adsorption ability of DGF could be attributed to more active sites on graphene surfaces, such as catechol groups resulting from the PDA polymerized on graphenenanosheets. DGF hybrids have a large amount of negatively charged oxygen functional groups, which are favorable for adsorption of cationic MB.

The adsorption isotherm is the most important parameter to describe the process of an adsorption system. Fig. 7 shows the adsorption systems of dye MB on the GF and DGF composite at different initial MB concentrations. The MB adsorption on different samples can be simulated by the Langmuir and Freundlich isotherm models,[16] which could be expressed as follows:

Langmuir isotherm model: $q_e = \frac{\mathrm{b}q_{max}C_e}{1+\mathrm{b}C_e}$

Freundlich isotherm model: $q_e = kCe^{1/n}$

whereq_e (mg/g) is the amount of MB adsorbed by the absorbents at equilibrium; C_e (mg/L) is the equilibrium concentration of MB; b is the constant of Langmuir; q_{max} (mg/g) is maximum adsorption capacity of MB calculated by the Langmuir isotherm

model; k and n are the Freundlich constants related to the adsorption ability.

Tab. 1 Adsorption kinetic parameters for MB adsorption on the DGF and GF composite

Adsorbent	Langmuir			Freundlich		
	q_{max} (mg/g)	b (L/mg)	R^2	k	n	R^2
GF	289.27	0.20	0.92	92.68	3.85	0.95
DGF	371.75	0.81	0.95	162.40	5.26	0.81

Tab. 1 summarizes the constants of Langmuir and Freundlich isotherm models and the calculated coefficients. It can be found that the maximum adsorption capacity of DGF is 371.75 mg/g, which is much higher than that of GF (289.27 mg/g). The regression coefficient R^2 of DGF calculated from the Langmuir model is much higher than that from the Freundlich model, indicating that the Langmuir isotherm model matches better with the experimental data. These results demonstrate that the adsorption of MB is a mono-molecule layer adsorption process and the adsorption takes place at the surface of DGF. However, the Freundlich isotherm model is more aligned with GF, which R^2 is higher than that of Langmuir model.

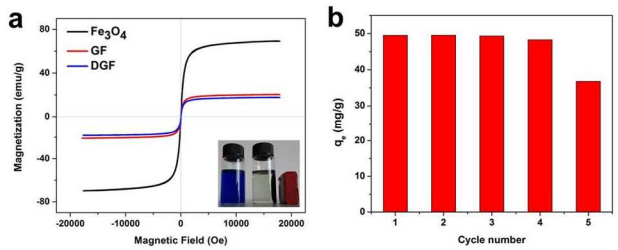

Fig. 8(a) Magnetic hysteresis loops of Fe_3O_4, GF and DGF. The inset picture shows aqueous solutions of MB before and after adsorption; (b) Adsorption capacity of MB on the DGF composite in 5 successive cycles of adsorption-desorption (initial MB concentration: 50 mg/L; temperature: 25 ℃; contact time: 20 min)

Fig. 8a shows the magnetic hysteresis loops of water-soluble Fe_3O_4 nanoparticles, GF and DGF. The magnetization loops are critical S-like curves. The saturation magnetization (Ms) of Fe_3O_4, GF and DGF is 69.6, 20.6 and 18.0 emu/g, respectively. All the samples show superparamagneticbehavior. The DGF has a lower value of Ms than that of GF and pure Fe_3O_4, which could be attributed to the relatively low amount of Fe_3O_4 on graphene (estimated Fe_3O_4 amount in DGF: 25%). The magnetic responsibility of adsorbent made it be quickly removed by an external magnetic field instead of the time-consuming process, such as sedimentation, centrifugation and filtration and can also be recycled many times by a simple and easy way.[16,18,21] As known, the cyclic utilization of the adsorbent is critical for the industrial applications. Fig. 8b shows the adsorption capacity of MB on the DGF composite in 5 cycles of adsorption-desorption process. After the adsorption of MB, the adsorbent could be quickly separated by a magnet. Then the hybrid could be desorbed by the ethanol and reused for the next absorption process. After five cycles, the absorption ability of DGF could decrease to 36.79 mg/g and the corresponding removal efficiency is 74%. On the other hand, even after 5 adsorption-desorption cycles, DGF composites still have better external magnetic response and could be removed by a magnet just in 1 min. This suggests that the close integration between graphene and Fe_3O_4 owing to the electrostatic interaction and hydrogen-bond interaction.

4. Conclusions

In summary, polydopamine-functionalized graphene-Fe_3O_4 (DGF) nanocomposites are successfully prepared by a facile solution method. The hybrids are used to absorb the MB dyes, and the adsorption mechanisms are investigated in detail. The Fe_3O_4 particles are adsorbed on the graphene surfaces by the electrostatic and hydrogen interactions. DGF and GF could absorb MB dyes in 5 min and could be separated by an external magnetic field in 1 minute instead of the time-consuming process such as centrifugation and filtration. The saturated adsorption capabilities for DGF and GF are individually 365.39 mg/g and 293.37 mg/g. The enhancement of adsorption capability could be ascribed to the functionalization of the polydopamine which not only endow abundant chemical groups for adsorption, but also could form adhesive coatings on the graphene to prevent the aggregation of graphene sheets and protects the stable structure of the hybrids. The magnetic capability of nanocomposites could also endow it recycling property. The removal efficiency of DGF could reach 74% even after 5 successive cycles of adsorption-desorption process. DGF could be used to remove the contaminants from water, which is very important for the water conservation. This study shows an easy way to fabricate reusable graphene based nanocomposites with high adsorption property. We believe that DGF will become a promising candidate for the water purification.

Acknowledgment

This work was supported by the National Natural Science Foundation of China (51173043, 21136006, 21236003，21322607), the Special Projects for Nanotechnology of Shanghai (11nm0500200, 12nm0502700), the Basic Research Program of Shanghai (13JC1408100, 13NM1400801), Program for New Century Excellent Talents in University (NCET-11-0641)，the Fundamental Research Funds for the Central Universities.

Notes and references

Key Laboratory for Ultrafine Materials of Ministry of Education, School of Materials Science and Engineering, East China University of Science and Technology, Shanghai 200237, China. Fax: +86 21 6425 0624; Tel: +86 21 6425 0949; E-mail: czli@ecust.edu.cn and zlingzi@ecust.edu.cn

1 T. Kuilla, S. Bhadra, D. H. Yao, N. H. Kim, S. Bose and J. H. Lee, *Prog. Polym. Sci.,* 2010, **35**, 1350.
2 X. Huang, Z. Y. Yin, S. X. Wu, X. Y. Qi, Q. Y. He, Q. C. Zhang, Q. Y. Yan, F. Boey and H. Zhang, *Small,* 2011, **7**, 1876
3 O. C. Compton and S. T. Nguyen, *Small*, 2010, **6**, 711
4 S. Stankovich, D. A. Dikin, R. D. Piner, K. A. Kohlhaas, A. Kleinhammes, Y. Y. Jia, Y. Wu, S. T. Nguyen and R. S. Ruoff, *Carbon*, 2007, **45**, 1558
5 H. Lee, S. M. Dellatore, W. M. Miller and P. B. Messersmith, *Science*, 2007, **318**, 426

6 I. Kaminska, M. R. Das, Y. Coffinier, J. Niedziolka-Jonsson, J. Sobczak, P. Woisel, J. Lyskawa, M. Opallo, R. Boukherroub and S. Szunerits, *ACS Appl. Mater. Interfaces.*, 2012, **4**, 1016

7 L. Q. Xu, W. J. Yang, K. Neoh, E. Kang and G. D. Fu, *Macromolecules*, 2010, **43**, 8336

8 L. P. Yang, J. H. Kong, W. A. Yee, W. S. Liu, S. L. Phua, C. L. Toh, S. Huang and X. H. Lu, *Nanoscale*, 2012, **4**, 4968

9 C. Cheng, S. Li, S. Q. Nie, W. F. Zhao, H. Yang, S. D. Sun and C. S. Zhao, *Biomacromolecules*, 2012, **13**, 4236

10 X. L. Hu, R. R. Qi, J. Zhu, J. Q. Lu, Y. Luo, J. Y. Jin and P. K. Jiang, *J. Appl. Polym. Sci.*, 2014, 39754

11 J. Ryu, S. H. Ku, M. Lee and C. B. Park,*Soft Matter.*, 2011, 7, 7201

12 H. K. He and C. Gao, *ACS Appl. Mater., Interfaces.* 2010, **2**, 3201

13 T. W. Lu, R. B. Zhang, C. Y. Hu, F. Chen, S. W. Duo and Q. H. Hu, *Phys. Chem. Chem. Phys.*, 2013, **15**, 12963

14 Z. S. Wu, W. C. Ren, L. Wen, L. B. Gao, J. P. Zhao, Z. P. Chen, G. M. Zhou, F. Li and H. M. Cheng, *ACS Nano*, 2010, **4**, 3187

15 Y. Y. Liang, Y. G. Li, H. L. Wang, J. G. Zhou, J. Wang, T. Regier and H. J. Dai, *Nat. Mater.*, 2011, **10**, 780

16 W. Fan, W. Gao, C. Zhang, W. W. Tjiu, J. S. Pan and T. X. Liu, *J. Mater. Chem.*, 2012, **22**, 25108

17 M. C. Liu, C. L. Chen, J. Hu, X. L. Wu and X. K. Wang, *J. Phys. Chem. C*, 2011, **115**, 25234

18 S. Bai, X. P. Shen, X. Zhong, Y. Liu, G. X. Zhu, X. Xu and K. M. Chen, *Carbon*, 2012, **50**, 2337

19 J. Su, M. H. Cao, L. Ren and C. W. Hu, *J. Phys. Chem. C*, 2011, **115**, 14469

20 F. J. Zhang, J. Liu, K. Zhang,W. Zhao, W. K. Jang andW. C. Oh, *Korean J. Chem. Eng.*, 2012, **29**, 989

21 G. Q. Xie, P. X. Xi, H. Y. Liu, F. J. Chen, L. Huang, Y. J. Shi, F. P. Hou, Z. Z. Zeng, C. W. Shao and J. Wang, *J. Mater. Chem.*, 2012, **22**, 1033

22 Y. H. Xue, H. Chen, D. S. Yu, S. Y. Wang, M. Yardeni, Q. B. Dai, M. M. Guo, Y. Liu, F. Lu, J. Qu and L. M. Dai, *Chem. Commun.*, 2011, **47**, 11689

23 J. J. Liang, Y. F. Xu, D. Sui, L. Zhang, Y. Huang, Y. F. Ma, F. F. Li and Y. S. Chen, *J. Phys. Chem. C*, 2010, **114**, 17465

24 X. Yang, C. L. Chen, J. X. Li, G. X. Zhao, X. M. Ren and X. K. Wang,*RSC Adv.*, 2012, **2**, 8821

25 J. H. Deng, X. R. Zhang, G. M. Zeng, J. L. Gong, Q. Y. Niu and J. Liang, *Chem. Eng. J.*, 2013, **226**, 189

26 J. H. Byeon, J. H. Park, K. Y. Yoon and J. Hwang, *Nanoscale*, 2009, **1**, 339

27 L. M. Malard, M. A. Pimenta, G. Dresselhaus and M. S. Dresselhaus, *Phys. Rep.*, 2009, **473**, 51

28 H. C. Gao, Y. M. Sun, J. J. Zhou, R. Xu and H. W. Duan, *ACS Appl. Mater. Interfaces.*, 2013, **5**, 425